Journal of Systems Architecture 176 (2026) 103814

Contents lists available at ScienceDirect

Journal of Systems Architecture

journal homepage: www.elsevier.com/locate/sysarc

Optimizing irrigation in peach trees by predicting trunk water potential using machine learning based on FloraPulse microtensiometers ☆

Yu Ye [a], María Fernanda García Cruz [a], Ricardo Javier Sendra Lázaro [a], Miguel A. Zamora-Izquierdo [a,*], Aurora González-Vidal [a], Pedro Nortes Tortosa [b], José Salvador Rubio-Asensio [b], María Fernanda Ortuño Gallud [b], Antonio F. Skarmeta [a]

[a] Department of Information and Communication Engineering, University of Murcia, Murcia, Spain
[b] Department of Irrigation, Centro de Edafología y Biología Aplicada del Segura CEBAS-CSIC, Murcia, Spain

ARTICLE INFO

Keywords:
Microtensiometer
Water stress
Machine learning
Long Short-Term Memory
Trunk water potential

ABSTRACT

Efficient water management in agriculture is a critical challenge to ensure sustainability, especially in water-constrained regions. Advanced technologies, such as FloraPulse microtensiometers, offer an innovative solution by enabling accurate, real-time monitoring of plant water status by measuring Trunk Water Potential (TWP). This information is essential for assessing water stress and optimizing irrigation decisions. This work is the first stage of an overall objective to predict the optimal timing and amount of irrigation. It is important to note that the current models were trained and tested using data from the 2023 season, when all trees were irrigated to 100% of ET_c. In this first phase, predictive models are developed that uses advanced Machine Learning (ML) and Deep Learning (DL) techniques to estimate TWP, providing a key tool to anticipate plant water stress as a function of climatic and edaphic variables. According to the initial comparison where ML models (RF, SVR and KNN) and DL model (LSTM) were implemented without using the previous TWP values as input to make the next hour prediction, the LSTM model outperformed the ML models, achieving average R^2=0.75, MAE=0.19 MPa and CVRMSE=19.22%. Using the lagged TWP values, the LSTM model showed a significant improvement, with average R^2=0.98, MAE=0.036MPa, and CVRMSE=4%. In addition, LSTM models with 6, 12 and 24 h prediction horizons were developed, all with R^2 greater than 0.89, MAE less than 0.12 MPa and CVRMSE less than 17%. These results allow the precise prediction of future TWP values and thus offer the design of more accurate and efficient irrigation systems.

1. Introduction

Agriculture plays a fundamental role in the transition to more sustainable systems, as it is responsible for more than 70% of global water withdrawals, making it the largest user of this resource worldwide. However, of these withdrawals, about 41% are not carried out in a way that is compatible with the maintenance of ecosystem services, representing a significant threat to biodiversity and natural resources [1,2]. As the demand for freshwater grows due to population increase, industrialization and agricultural expansion, particularly in arid and semi-arid regions such as the Mediterranean basin, competition between these sectors (agriculture, industry and human supply) generates unprecedented pressure on water resources [3,4]. This scenario poses a critical challenge; to ensure sustainable agricultural production without compromising water availability for other uses.

In this context, it is essential to implement agricultural practices that promote water conservation, especially in high-value crops, such as outdoor fruit orchards, which are exposed to various adverse environmental conditions throughout their growth cycle, drought being one of the most severe, with negative effects on production [5]. Among these practices, drip irrigation has positioned itself as an efficient alternative, allowing a more precise distribution of water and reducing losses due to evaporation and runoff. However, optimizing water use in agriculture requires not only the implementation of advanced irrigation technologies, but also the development of tools to monitor and manage the water status of crops in real time. This is particularly relevant in a global scenario where the growing scarcity of freshwater is one of the most serious constraints to sustainable agricultural production.

Spain is one of the main players in world peach (*Prunus persica* (L.) Batsch) production, occupying second place globally thanks to

☆ This article is part of a Special issue entitled: 'EDiS2024' published in Journal of Systems Architecture.

* Corresponding author.
E-mail address: mzamora@um.es (M.A. Zamora-Izquierdo).

https://doi.org/10.1016/j.sysarc.2026.103814
Received 23 June 2025; Received in revised form 23 March 2026; Accepted 22 April 2026
Available online 7 May 2026

the extension and productivity of its plantations. Peach production is mostly concentrated in the Mediterranean area, where factors such as climate and technical expertise in crop management have boosted the sector's competitiveness. In 2022, the Region of Murcia stood out as the main peach producer in Spain, with a volume of 190, 195 tons, equivalent to 33% of the national total [6].

However, this leading position faces significant challenges related to the availability of water for irrigation. In Mediterranean areas, increasing water resource constraints are aggravating the risk of irrigated land loss, which could compromise not only agricultural productivity but also the economic sustainability of the region. Faced with this problem, a viable strategy to mitigate the impact of water scarcity is to reduce the amount of water applied at certain critical periods of the year, without significantly affecting yields and fruit quality. This approach not only increases water use efficiency, but also contributes to water conservation, ensuring the viability of the peach crop in the face of climate change scenarios and increasing water limitations.

Accordingly, a key question that guides the present study arises: how to determine how much to reduce the amount of water applied in irrigation without inducing water stress in the crop? This question is especially critical in the case of peach trees, since water stress, if not adequately controlled, can affect both yield and fruit quality, negatively impacting crop profitability. The answer to this problem is not simple, since it depends on a series of interrelated factors, such as climatic conditions, soil characteristics, phenological stage of the crop and specific management objectives.

To address this challenge, advanced tools are needed to monitor crop water status accurately and in real time. Technologies such as dendrometers, which measure fluctuations in trunk diameter, or sap flow sensors, which record water transport within the tree, provide valuable information on physiological changes associated with water stress [7]. However, these tools have certain limitations, such as sensitivity to external factors and high implementation costs in commercial orchards.

In this context, Microtensiometers (MT), such as the FloraPulse, have emerged as a promising solution; they play a key role by continuously integrating soil water availability and atmospheric demand throughout all phenological phases of the crop [8–11]. These devices directly measure Trunk Water Potential (TWP or ψ_{trunk}); which reflects the water tension within the trunk, quantifying the pressure required to mobilize plant sap through the trunk. Unlike traditional methods, such as the Scholander pressure chamber [12], which measures Stem Water Potential (SWP or ψ_{stem}), MTs allow continuous and non-destructive measurements to be obtained, facilitating the integration of data into automated irrigation systems [13].

The final decision on when and how much to irrigate requires an integration of multiple sources of information, such as sensor-generated data, current and predicted weather conditions, and knowledge of crop phenological conditions [14]. Moreover, this decision must be dynamic and adaptable to changing environmental scenarios, which demands tools capable of processing large volumes of data and providing accurate recommendations in real time.

In this regard, the use of predictive models based on Artificial Intelligence (AI) and Machine Learning (ML) represents a key advance. These techniques make it possible to analyze data from sensors, combine them with climatic and phenological variables, and generate reliable predictions that help optimize water management decisions. Therefore, AI-based solutions will help farmers produce more with fewer resources, improve the quality of their crops, and reduce the time it takes for their products to reach the market [15]. In this context, the present study explores the use of ML models to forecast TWP using environmental, soil, and irrigation data. Consequently, the main contributions of the study are as follows:

- In the first phase of the project, embodied in Cruz et al. [16], a ML-based predictive model was developed to estimate TWP using data from FloraPulse sensors, climatic variables, Soil Water Content (SWC) and indices such as crop coefficient (K_c). This model had the ability to predict TWP 15 min in advance, providing an initial tool to anticipate water stress in real time.
- The present study extends the previous research with the objective of extending the predictive capacity of the 1-hour model up to 24 h, this improvement will allow farmers to anticipate more accurately the evolution of the water stress of their crops, optimizing irrigation scheduling based on TWP predictions and future environmental conditions.
- Comparative evaluation of several ML algorithms for predicting plant water status in orchard conditions.
- Additionally, this work contributes to developing a broader digital platform that supports irrigation management. Within this platform [17], predictive models, such as the one proposed in this study, will serve as components of a future Marine-Agricultural Digital Twin framework, where multiple data sources and models will be integrated to simulate crop water dynamics and evaluate irrigation scenarios.

However, the dataset used for model training and testing was collected during the 2023 growing season under full irrigation, ensuring homogeneous, well-watered conditions. The models' predictions of TWP are accurate within this range. Nevertheless, their performance under deficit irrigation or drought conditions has not yet been validated. The current model should therefore be interpreted primarily as a predictor of TWP dynamics under optimal irrigation rather than as a fully validated irrigation optimization tool.

2. Related work and motivation

2.1. Related work

Precision agriculture has advanced the monitoring of tree water status, providing detailed data that improves irrigation management and water optimization in agriculture through the implementation of advanced sensors and technologies that optimize irrigation, improving crop sustainability. The growing demand for automated and non-invasive solutions has driven the development of continuous plant-based sensors designed to provide real-time data on tree water status and effectively integrate into autonomous irrigation systems. Several studies have explored promising alternatives, such as Barriga et al. [18], where a MT (leaf turgor pressure sensor) based approach was used to assess water stress in fruit trees. This study proposes an innovative system based on ML and the Internet of Things (IoT) to continuously measure leaf turgor pressure and assess the water status of crops, especially citrus, in deficit irrigation scenarios. The system exhibits high accuracy, with an F1 score of 99%. This allows optimizing irrigation scheduling, adjusting to crop water requirements, and applying efficient irrigation strategies under water shortage conditions. It was noted that continuous monitoring with physiological sensors allows better predictions than methods based only on soil moisture or evapotranspiration. The study suggests that the combination of sensors and predictive models can improve irrigation scheduling.

Considering the findings of multiple studies, including those by Blanco and Kalcsits [19,20], which have demonstrated strong correlations between TWP measured with MT and SWP obtained using the pressure chamber [14,21], TWP is recognized as a direct and reliable measure of water status in woody perennial plants, as it accurately quantifies the water tension within the plant (MPa), reflecting the internal water balance of trees and their response to environmental conditions and irrigation [14,22–24]. Historically, measurement of this indicator of tree water status has been performed using the Scholander pressure chamber [12], a standard, but laborious and destructive method, limiting its application in making immediate irrigation decisions [12,25–27]. To measure SWP, a healthy leaf not exposed to direct sunlight is selected and covered with black plastic and aluminum foil for two hours to stop transpiration and allow the leaf water potential to reach equilibrium with the trunk. Although this indicator integrates soil, plant and atmospheric factors, its main limitation lies in the time required for measurement and its discontinuous nature. Therefore, MTs have emerged as a viable alternative for continuous TWP measurement. These devices employ microelectromechanical pressure sensors inserted into the tree trunk, continuously measure water tension, which, as mentioned, allows obtaining accurate and real-time measurements of water potential [28,29]. Unlike conventional methods, MTs facilitate constant monitoring and have shown positive correlations with values obtained using the pressure chamber [19,21]. However, further research is still required on their behavior under different environmental conditions and their stability over several growing seasons [14,30].

As mentioned above, the incorporation of AI and ML agriculture has facilitated a significant transformation in agricultural management, offering predictive tools that, for example, make it possible to anticipate water stress and optimize irrigation planning. Recent studies have demonstrated the potential of learning-based approaches to integrate heterogeneous agricultural data sources and improve the prediction of crop water status and irrigation management decisions [31–33]. Mortazavi et al. [34] implemented ML models to predict SWP in pistachio and almond orchards using meteorological, thermal and multispectral data. Supervised models, such as Random Forest (RF), achieved accuracy higher than 79%, highlighting 88% in pistachios and 89% in almonds. The results showed that climatic variables and canopy temperature were crucial for predicting SWP, providing an effective tool for efficient water management in agriculture. The study suggests that data-driven predictive models can improve water management and be scalable to other crops.

On the other hand, Salek et al. [35] demonstrated that hyperspectral images combined with ML algorithms such as Artificial Neural Networks (ANNs) can detect drought stress levels in safflower before visible symptoms appear. ANNs achieved high classification rates, with F1 scores of 92.22%, 96.01% and 96.47% in distinguishing stress levels (no stress, mild and severe). It could be concluded that ANN models clearly described the progression of leaf stress in different genotypes and hyperspectral imaging showed great potential for assessing drought stress, improving prediction and monitoring in this crop.

Despite progress in plant-based sensing and irrigation monitoring, existing approaches have several limitations. Many studies focus on monitoring crop water status rather than predicting it. Others rely on limited input variables or short prediction horizons, which restricts their ability to capture the complex interactions between environmental conditions, soil water availability, irrigation management, and plant physiology. Furthermore, comparative evaluations of ML models for predicting plant water status remain limited. This study evaluates multiple ML algorithms to predict tree TWP using environmental, soil, irrigation, and plant-based sensing data across different forecasting horizons to address these gaps.

2.2. Motivation

The studies reviewed provide evidence of how advanced technologies and predictive models can be integrated to address water management challenges in modern agriculture. ML systems and innovative tools such as FloraPulse MTs stand out for their ability to optimize irrigation scheduling, promote sustainability and ensure productivity in high-value crops such as peaches. In this sense, the proposal presented in this research is based on using the FloraPulse MT as a data source for ML models to predict the TWP of peach trees and with this identify the water status of the crop. As noted above, in the first phase of the project, embodied in Cruz et al. [16], an ML-based predictive model was developed to estimate TWP using data from FloraPulse sensors, climatic variables, SWC, and indices such as K_c. This model had the ability to predict TWP 15 min in advance, providing an initial tool to anticipate water stress in real time. In this research, different prediction models were compared, highlighting the performance of the RF algorithm, which showed a correlation higher than 0.96, confirming its viability as a tool for decision making in irrigation management. In this second phase, the previous research is extended with the objective of extending the predictive capacity of the 1 h model to 24 h. To the best of our knowledge, this approach represents an innovative contribution in the prediction of indicators related to plant water status, since, unlike previous studies that approach the problem as a classification task, we treat water status with exact values. This method allows a more accurate and detailed estimation, which improves decision making and optimizes water use in agricultural management.

3. Material and methods

This research presents the development of an advanced system for the evaluation and estimation of peach tree water status, integrating data obtained from FloraPulse MT, climatic variables, soil parameters and phenological indices of the crop. This system is based on the implementation of ML algorithms for accurate TWP prediction. In the following, the context of the experimental crop, the methods used for data acquisition, the configuration and architecture of the ML model, as well as the experiments performed to evaluate and validate its performance are described in detail.

3.1. Field conditions

The experiment was carried out in a 2 ha peach orchard located in Jumilla (Murcia, Spain) (38° 29′ 34.29″ N, 1° 21′ 46.76″ W) during the 2023 growing season, from March to October. The climate of this region is characterized by dry summers and cold winters. In the last 12 years the average precipitation was 267.3 mm, and the average Crop Reference Evapotranspiration (ET_o) calculated using the Penman-Monteith equation [36] was 1320 mm, these data were obtained from the meteorological station JU62 (Jumilla, Miraflores) of the Agrometeorological Information System of the Region of Murcia (SIAM).

The trees were planted in 2010, using the Grocivac 2 variety (IVIA) on GF677 rootstock at a distance of 5.5 m × 3 m. Two lines per row were installed for irrigation (AZUD Premier PC AS 16/1.1 mm, Murcia, Spain), buried 30 cm, and with drippers of 2.3 L/h, spaced 0.6 m apart. The irrigation lines were separated 1 m from the trunk. Although the plot was divided into 4 treatments with 2 replicates each, during the 2023 season all trees were irrigated with the same amount of water. The irrigation dose was calculated to satisfy the maximum crop requirement (ET_c) during the whole growing season, where $ET_c = ET_o * K_c$ [36], K_c being the peach crop coefficient indicated by Girona et al. [37].

3.2. Sensor to measure TWP

The FloraPulse MT (FloraPulse, Davis, CA, USA) is a sensor implanted directly into the trunk of trees (see Fig. 1) that accurately and continuously measures TWP. It quantifies water tension, which indicates the strength with which the woody tissue retains water. Higher tension indicates less free water in the stem, which occurs under conditions of water scarcity. This measurement covers the entire path of water through the plant, from its absorption in the roots, which take up available water in the soil, to its transport through the xylem in the stem, and its distribution to the leaves and fruits, where it finally evaporates into the air through the process of transpiration [19]. This continuous flow is essential to maintain the plant's water balance and physiological functioning, and the FloraPulse MT allows the variations in this process to be accurately quantified. This device uses advanced tensiometry technology to provide real-time data on plant water status. For a detailed explanation on the theory of tensiometry, it is recommended to consult Pagay et al. [29]. In addition, Black

Fig. 1. Position of the FloraPulse on each tree.
Source: Irrigation Department, CEBAS-CSIC, Murcia.

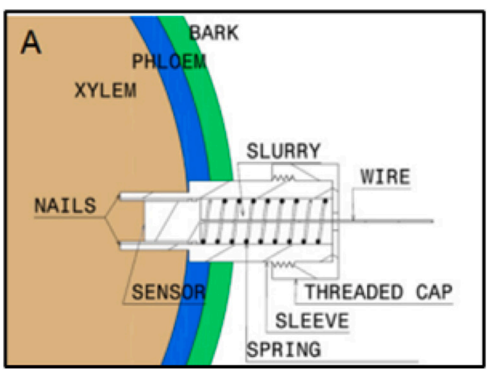

Fig. 2. MT installation scheme.
Source: [19].

et al. [38] provides technical information on the design, fabrication, calibration and laboratory testing of the MT sensor, evaluating its performance under controlled conditions. Also, Lakso et al. [39] provides a comprehensive description of the characteristics and operation of the MT sensor. The installation of the sensor was done according to the manufacturer's recommendations and taking into account the scheme presented by Blanco and Kalcsits [19] (see Fig. 2), where it is described that the MT must be correctly embedded in the tree trunk, since an erroneous or loose contact between the sensor and the trunk can result in unstable and variable measurements.

It should be noted that the daily minimum TWP values obtained from the MT are more accurate indicators of immediate water stress compared to the maximum values, due to their greater sensitivity to daily meteorological conditions. These minimum values are usually recorded in the afternoon, when atmospheric demand is highest [20]. Based on this information, critical TWP limits were established to ensure adequate fruit development. These values, detailed in Table 1, serve as key parameters in the calibration of the mathematical model.

3.3. Field measurements and data acquisition

During the experimental period, agrometeorological data (air temperature, T; relative humidity, RH; precipitation, P; solar radiation, Rs; wind speed, U; vapor pressure deficit, VPD) were taken from the meteorological station JU62 belonging to SIAM because it is located in an area close to the experimental plot. ET_o was calculated following the Penman-Monteith equation [36]. A Python script is programmed to collect and compute the above data.

Table 1
Critical values or limits of the TWP for optimal peach fruit development.

Fruit development stage	Limit TWP (MPa)
Cell division	−0.9
Hardening of the stone	−1.8
Cell expansion	−1.0
Postharvest	−1.8

Soil water status was continuously monitored by SWC measurements. In the second half of March 2023, eight Sentek Drill and Drop probes (Sentek Sensor Technologies, Sydney, Australia) were installed in the field, allowing SWC to be measured at multiple depths, each ranging from 0.1 to 0.9 m. Installation was performed on eight representative trees at approximately 0.75 m from the trunk. At this point it was considered that, although the root system of the peach tree is highly branched, the absorbing roots do not go deeper than 0.45 m in drip irrigation [40], so the SWC measurement used in the model is the normalized value between 0.35–0.55 m.

In the selected trees, FloraPulse MTs were installed embedded in the trunk, away from direct sunlight. Both the soil humidity probes and the MTs were connected to a datalogger (Nutricontrol, luxar lite, Murcia, Spain) that allows the transmission of these measurements in real time, values were read every 5 min and the measurement was recorded every 15 min. Fig. 3 shows the distribution map of peach trees selected for the installation of FloraPulse MTs and Sentek Drill and Drop moisture probes.

In order to verify the correlation between TWP reported by MT and SWP measured with a pressure chamber, and thus confirm the reliable use of MT as a tool for continuous monitoring of tree water status, comparative measurements were carried out under field conditions [14,20]. Midday SWP measurements are made twice a month using a Scholander-type pressure chamber (Model 600, PMS Instrument Company, Albany, OR, USA). Two mature leaves from three different trees were selected for measurement for each experimental unit. The leaves were covered with aluminum-coated plastic bags at least one hour before measurements, which were carried out between 12:00 and 14:00 h solar. In addition, SWP of the above mentioned trees were measured from sunrise to sunset, at two-hourly intervals throughout two days (see Fig. 4).

3.4. Data processing and study workflow

Fig. 5 depicts the workflow of this study. The input variables are climatic variables (T, P, RH, Rs, U, VPD and ET_o), K_c, SWC (0.35–0.55 m), applied irrigation (IR), the equation:

$$\text{hour\_sin} = \sin\left(\frac{2\pi \times \text{hour}}{24}\right) \tag{1}$$

is used to transform the hour of the day (named as hour_sin) to maintain continuity and prevent abrupt jumps between the highest and lowest values (e.g., hour 23 to hour 0). The previous (lagged) values of the input values are also included and prepared as sequence data to train the models since they can be used as predictors to capture the temporal dependency inherent in plant water status dynamics. The climatic variables, K_c and hour_sin are the same for all peach trees. However, the variables SWC, IR and TWP are measured individually. It should be noted that two versions of the training methods were first tested with the next hour forecast. One with its own previous TWP values and the other without. The reason for this experiment is that we want to investigate the performance of using only climatic, SWC and IR

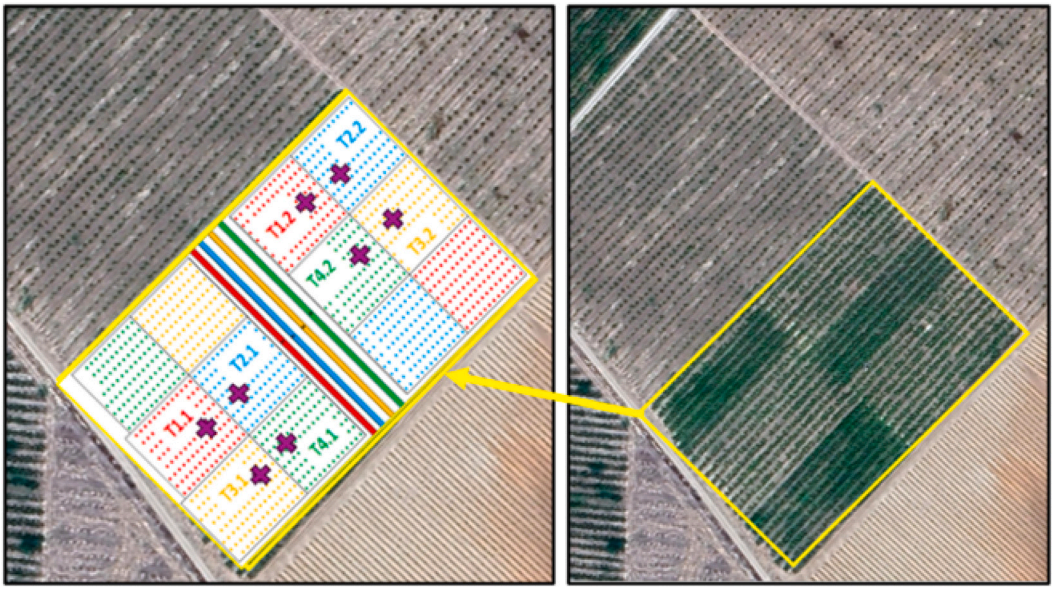

Fig. 3. Location of the experimental orchard. The x's represent the eight trees selected for sensor installation.

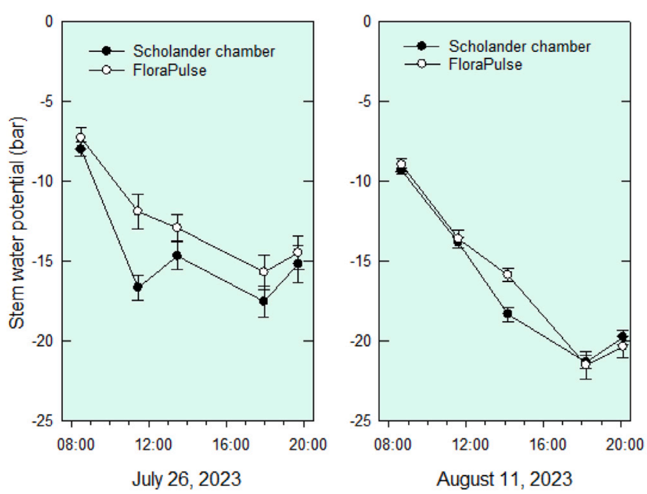

Fig. 4. Diurnal course of SWP measured using FloraPulse MT and Scholander chamber over two days of the experimental period. Vertical bars on points are ±S.E. of the mean.

variables to predict TWP values, also to compare the improvement of including the own lagged output values, and then decide which version to proceed with. All variables have been resampled to hourly data and scaled using the equation:

$$X_{\text{std}} = \frac{X - X_{\min}}{X_{\max} - X_{\min}} \tag{2}$$

where X is the original value, X_{std} the standardized value and X_{min} and X_{max} are the feature range (i.e., 0 to 1).

The period of the dataset is from the month of June to September of the year 2023, when the experiment was conducted on eight peach trees. However, due to technical and maintenance problems, some sensors did not work properly during some periods. Specifically, the data of tree T1.1. starts from June 21, 2023 10:00, tree T4.2. starts from July 26, 2023 13:00, and tree T3.2. was removed due to a possible failure of its SWC sensor. Data from different peach trees are stacked and each one of them are encoded with an extra column in order to have a categorical feature. Observations with missing values are removed. Fig. 6 shows the preprocessed time series data used for this study. Each series is divided into a training set (70%) to train the models and a test set (30%) to evaluate the performance of those models.

On the other hand, a first comparison between ML and DL models was made for the 1 h forecast horizon (with and without own lagged TWP values). However, only DL models, implemented with Long Short-Term Memory (LSTM) algorithm, were developed for the remaining horizons (i.e. 6 h, 12 h and 24 h). The main reason for this decision is that the TWP values have very strong patterns of time series data and LSTM were specifically designed to process and predict this type of data. Other similar studies have already come to this conclusion [41, 42]. The first comparison also serves as proof of this fact.

Finally, fixed seed values are used for reproducibility when a function could produce random results (123 for random data splitting and 1234 for LSTM model hyperparameter tuning). All data and code used in this study are available at: https://github.com/yuye188/FloraPulseModels.

3.5. ML and DL algorithms

Prior to the implementation of ML and DL models, it is imperative to establish the fundamentals of their utilization. The primary objective of this study is to develop predictive models capable of estimating TWP efficiently, thereby facilitating the optimization of irrigation strategies. Given the complexity of plant responses to climatic and irrigation variables, regression-based models were deemed the most suitable approach to capture these relationships. The ability to predict TWP with high accuracy is essential to prevent unnecessary water stress and optimize water use, particularly in regions with limited water resources. In addition, data preprocessing plays a key role in the effectiveness of these models. Since some ML techniques, such as Support Vector Machine (SVM), are very sensitive to data scaling, normalization techniques were applied to ensure consistency of all input features. In addition, feature engineering steps were carried out to improve model interpretability and performance. The subsequent section will present the ML and DL models applied in this study, along with the hyperparameter tuning process carried out to improve their predictive capabilities.

To ensure fair benchmarking, all models were trained and evaluated under the same data splits and experimental conditions. All ML models were implemented on Python using the following libraries: Keras [43] and Scikit-learn [44]. All computations for the ML tecnics were running

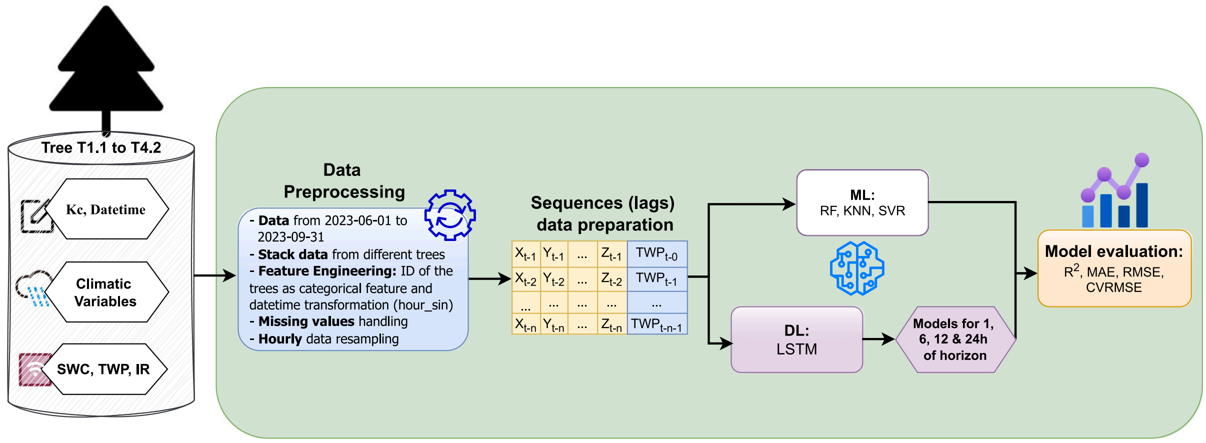

Fig. 5. Flowchart of the study.

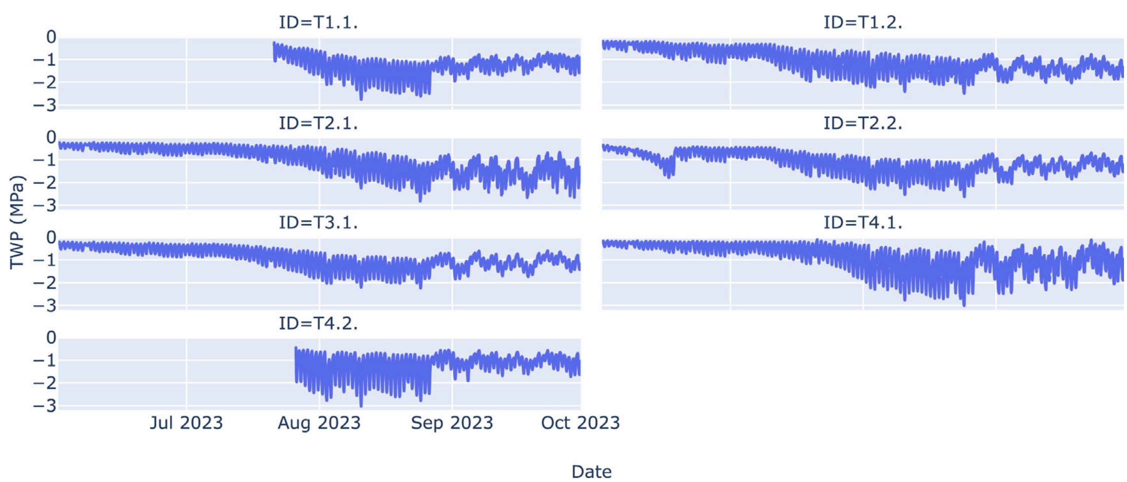

Fig. 6. Time series data of the peach trees.

in a workstation over Python 3.12.3 with the following features: 12th Gen Intel(R) Core(TM) i7-12700H 2.30 GHz and 16 GB of RAM. For the DL model the computations were running in a workstation over Python 3.11.2 (AMD Ryzen 7 3700X 8-core processor at 3.59 GHz and 16 GB of RAM). The models used in this study are detailed below, as well as the hyperparameters optimization.

3.5.1. Random forest regressor

RF is an ensemble learning method that constructs multiple decision trees and outputs the mode of the classes (classification) or the mean prediction (regression) Breiman [45]. The model introduces randomness in the selection of features, which helps in reducing overfitting and improving generalization. Instead of selecting the best feature to split a node across all features, RF searches for the best feature among a random subset, increasing model diversity and robustness.

The hyperparameters tested in this work are:

- **Number of Trees in the Forest** (*n_estimators*): Determines how many decision trees are created in the ensemble. More trees generally improve performance but increase computational cost. Tested values: {100, 300, 500}.
- **Maximum Depth of the Trees** (*max_depth*): Controls how deep each tree can grow. A greater depth allows trees to capture more complex patterns but increases the risk of overfitting. Tested values: {10, 15, 20}.
- **Minimum Samples per Split** (*min_samples_split*): Specifies the minimum number of samples required to split a node. Lower values allow deeper trees, while higher values prevent overfitting. Default value used.
- **Minimum Samples per Leaf** (*min_samples_leaf*): The minimum number of samples that must be in a leaf node. Increasing this value reduces the model complexity. Default value used.
- **Bootstrap Sampling** (*bootstrap*): Determines whether bootstrap sampling is used when building trees. When set to True, each tree is trained on a random sample with replacement. Default value used.

The rest of the parameters remain at their default values.

3.5.2. Support vector regressor

SVM are powerful supervised learning models that can be used for classification and regression Cortes and Vapnik [46]. SVMs work by finding a hyperplane that best separates the data into different classes. The optimization problem solved by SVM is formulated as:

$$\min_{w,b} \frac{1}{2}\|w\|^2 \quad \text{subject to } y_i(w \cdot x_i + b) \geq 1, \forall i. \tag{3}$$

To handle non-linearly separable data, SVMs use kernel functions (see Fig. 7), such as:

- **Linear Kernel**: $K(x, y) = x \cdot y$
- **Polynomial Kernel**: $K(x, y) = (x \cdot y + c)^d$
- **Radial Basis Function (RBF) Kernel**: $K(x, y) = e^{-\gamma\|x-y\|^2}$
- **Sigmoid Kernel**: $K(x, y) = \tanh(\alpha x \cdot y + c)$

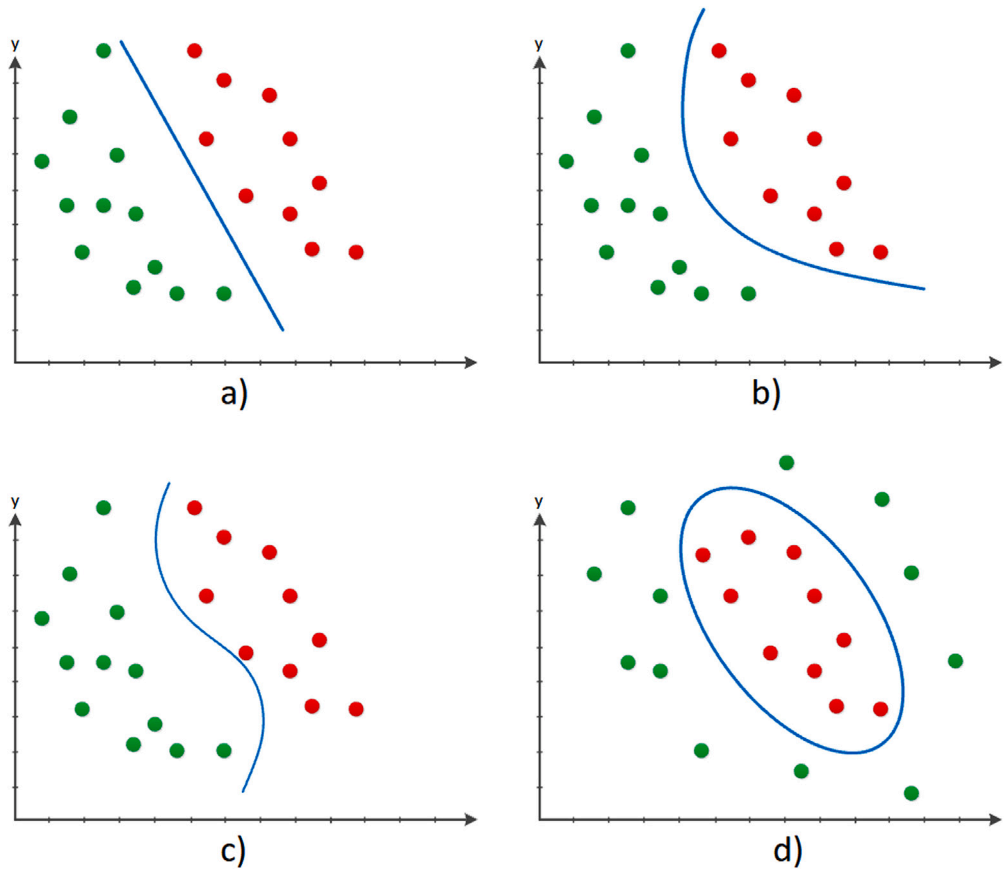

Fig. 7. Different kernel functions in SVM: (a) Linear Kernel, (b) Polynomial Kernel, (c) RBF Kernel, (d) Sigmoid Kernel.
Source: The kernel representations shown are adapted from Bellido-Jiménez et al. [47].

The choice of kernel influences the model's ability to capture complex decision boundaries. Hyperparameters such as the regularization parameter (C) and kernel coefficient (γ) are crucial in tuning SVM performance.Hyperparameters such as the regularization parameter (C), kernel coefficient (γ), and epsilon (ϵ) are crucial in tuning SVM performance. The hyperparameters tested in this work are:

- **Regularization Parameter (C)**: Controls the trade-off between achieving a low error and maintaining a small margin. Tested values: {0.1, 1, 10, 100}.
- **Epsilon (ϵ)**: Defines a margin of tolerance where predictions are not penalized. Useful in regression tasks. Tested values: {0.01, 0.1, 0.2}.
- **Kernel Type**: Defines the transformation applied to the input space. Tested values: {Linear, Polynomial, RBF}.

The rest of the parameters remain at their default values.

3.5.3. K-nearest neighbors

K-Nearest Neighbors (K-NN) is a simple, non-parametric algorithm used for classification and regression. The technique was first introduced by Cover and Hart [48]. The principle behind K-NN is that similar instances exist in close proximity in the feature space. Given a test instance, K-NN finds the k closest training samples using a distance metric. For classification, the label is determined by majority voting among the k nearest neighbors, while in regression, the average of the k nearest values is used.

The choice of distance metric significantly impacts the performance of K-NN. Commonly used distance metrics include:

- **Euclidean Distance**: Effective when data is well scaled.
- **Manhattan Distance**: Measures distance by summing absolute differences, useful for grid-based data.
- **Minkowski Distance**: A generalization of Euclidean and Manhattan distances, where the parameter p determines the form.
- **Hamming Distance**: Used for categorical data, measuring the number of differing elements.

The appropriate choice of distance metric depends on the nature of the data and feature scaling. Poorly scaled data can distort distances, leading to suboptimal classification or regression performance.

The hyperparameters tested in this work are:

- **Number of Neighbors ($n\_neighbors$)**: Defines how many neighboring points are used to make a prediction. Tested values: {7, 9, 11}.
- **Weighting Function ($weights$)**: Determines how neighbors contribute to the prediction. Options tested: {Uniform (all neighbors contribute equally), Distance-based (closer neighbors have more influence)}.
- **Algorithm Used ($algorithm$)**: Defines the method used to compute nearest neighbors. Tested values: {Auto, Ball Tree, KD Tree, Brute Force}.

The rest of the parameters remain at their default values.

3.5.4. Long short-term memory

LSTM is a variant of Recurrent Neural Networks (RNNs), specifically designed to process and predict time series data. Introduced in 1997 Schmidhuber et al. [49], LSTM overcomes the long-term dependency problem commonly found in traditional RNNs. It contains specialized units called memory cells that can store information over long periods of time. This capability allows LSTM to retain and use past data from a sequence, making it particularly effective for tasks involving sequential or time-series data.

LSTM uses three types of gates to regulate the flow of information: input gate (i_t), forget gate (f_t), and output gate (o_t), which can be expressed as follows:

$$f_t = \sigma(W_f \cdot h_{t-1} + W_f \cdot x_t + b_f), \tag{4}$$

$$i_t = \sigma(W_{ih} \cdot h_{t-1} + W_{ix} \cdot x_t + b_i), \tag{5}$$

$$\tilde{c}_t = \tanh(W_{\tilde{c}h} \cdot h_{t-1} + W_{\tilde{c}x} \cdot x_t + b_{\tilde{c}}), \tag{6}$$

$$c_t = f_t \cdot c_{t-1} + i_t \cdot \tilde{c}_t, \tag{7}$$

$$o_t = \sigma(W_{oh} \cdot h_{t-1} + W_{ox} \cdot x_t + b_o), \tag{8}$$

$$h_t = o_t \cdot \tanh(c_t). \tag{9}$$

where σ and tanh are activation functions; W_f and b_f are the weights and bias for f_t; h_{t-1} is the previous hidden state, and x_t is the current input. The cell state c_t is updated by combining the old cell state and the new candidate values $\tilde{c}_t$. o_t controls which parts of the c_t contribute to the hidden state h_t that is passed to the next time step. Finally, h_t is updated.

In this study, since the data were collected from different trees representing similar time series, the embedding layer was used as the first layer of the LSTM model architecture to increase the generalizability of the model (i.e., capable of making predictions for different trees). In the Keras implementation, the embedding layer is used to convert integer-coded categorical data (in this case, the tree ID) into dense vector representations.

The hyperparameters tested for the LSTM model were: the embedding dimension (from 4 to 20 with a step of 4), the number of neurons for the first LSTM layer (from 16 to 128 with a step of 8), the number of neurons for the second LSTM layer (from 8 to 64 with a step of 4), and the learning rate [0.0001, 0.001, and 0.01].

3.6. Evaluation metrics

Coefficient of determination (R^2), Mean Absolute Error (MAE), Root Mean Square Error (RMSE) and the Coefficient of Variation of the Root Mean Square Error (CVRMSE) or Normalized Root Mean Square Error (NRMSE) are used to evaluate model performance, which are expressed as follows:

$$R^2 = \frac{\left(\sum_{i=1}^{n}(y_i - \bar{y})(Y_i - \bar{Y}_i)\right)^2}{\sum_{i=1}^{n}(y_i - \bar{y})^2 \sum_{i=1}^{n}(Y_i - \bar{Y}_i)^2} \tag{10}$$

$$MAE = \frac{1}{n}\sum_{i=1}^{n}|y_i - Y_i| \tag{11}$$

$$RMSE = \sqrt{\frac{1}{n}\sum_{i=1}^{n}(y_i - Y_i)^2} \tag{12}$$

$$CVRMSE = (\frac{RMSE}{\bar{y}}) \times 100 \tag{13}$$

where n is the number of data points, y_i and Y_i present the observed (real) and predicted value of the ET_0 for the ith data point (day); $\bar{y}$ and $\bar{Y}$ are the mean of the observed and predicted values of y and Y. These evaluation metrics are widely used in regression and forecasting studies. Together, they provide complementary information about prediction accuracy and model performance. Moreover, the selected algorithms represent diverse machine learning approaches, including instance-based learning (KNN), kernel-based methods (SVR), ensemble methods (RF), and deep learning models (LSTM). This allows for a comprehensive comparison of predictive capabilities.

4. Results

After reviewing the models and datasets used in this study, we now proceed to analyze the results obtained from the experiments, which are divided into two sections: (i) models that do not include previous TWP values as input, and (ii) models that include previous TWP values. The main reason for this decision, as mentioned above, is to investigate how well the models can perform in predicting the TWP of a new peach tree when the FloraPulse sensor is not available. Furthermore, it will be further explored when the FloraPulse sensor data is present in order to make the best use of it.

4.1. Models without TWP lags

In order to determine the optimal number of lagged values for preparing the sequence data, a cross-correlation was first performed. Cross-correlation is a statistical measure widely used in ML and signal processing to quantify the similarity or relationship between two time series at different temporal offsets (lags). By systematically shifting one series relative to the other, cross-correlation identifies the time lag at which the two series have the strongest linear relationship. This technique is particularly valuable for uncovering temporal dependencies and patterns in datasets, allowing to better understand how past observations influence current or future outcomes. In ML, cross-correlation helps in selecting meaningful time-lagged predictors, thereby enhancing model accuracy and interpretability. Fig. 8 shows the cross-correlation between the lagged features and the target variable (FloraPulse), and Table 2 presents the minimum and maximum point of each variable and the corresponding value. Analyzing these results, we highlight several notable insights:

- Climatic variables, such as ET_o, Rs, T, U, and VPD, show optimal correlation lags predominantly around midday, approximately 8 to 12 h.
- Variables related to irrigation exhibit varying lags depending on their nature: IR shows a shorter lag of 8 h, while P demonstrates a longer lag of approximately 17 h.
- Lastly, SWC and RH have immediate or minimal lag correlations.

These findings align with biological expectations of the tree cycle. Irrigation typically requires between 6 and 10 h to influence plant water status, considering the response time between irrigation application and observable variation in TWP, determined mainly by soil type and its infiltration capacity [50]. Precipitation, being superficial, takes longer to impact the plant significantly, resulting in a longer lag. In contrast, climatic variables tend to affect plants within the same daily cycle.

In general, we have chosen a uniform lag of 12 h for all variables, as most of the variables have their maximum and minimum correlation (positive or negative) in this range. This decision simplifies the modeling process and captures daily cyclical patterns, while also minimizing potential noise introduced by over-extended lags in the ML models.

The results of tuning each hyperparameter for each model are presented in Table 3. The model evaluation results of the ML and LSTM models in the test set of each tree are shown in Table 4. It can be seen that LSTM outperforms all ML models, achieving R^2 = 0.754 with the lowest average MAE, RMSE and CVRMSE values of 0.191 MPa, 0.231 MPa and 19.222%, respectively. SVR has the highest errors (MAE = 0.220 MPa, RMSE = 0.279 MPa and CVRMSE = 22.925%), indicating difficulty in capturing the underlying patterns. RF and KNN show moderate performance but do not outperform LSTM. Regarding the trees, T4.2 shows the best prediction results among all models, while T4.1 is the most challenging with the highest errors.

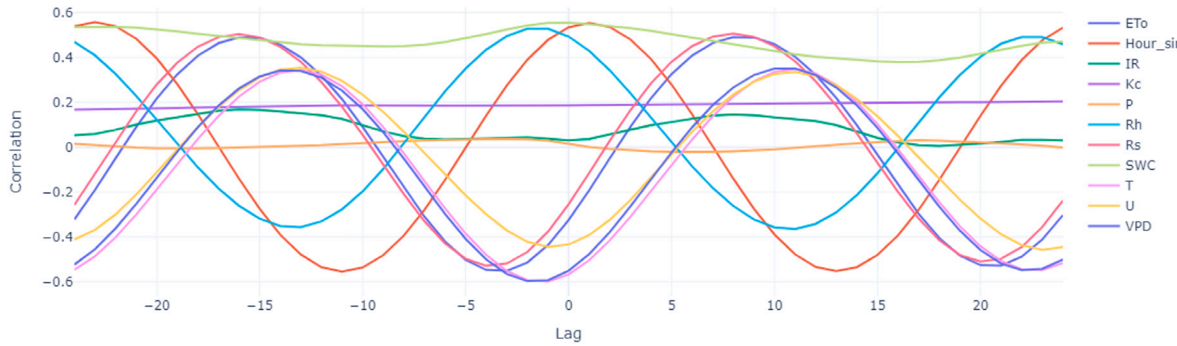

Fig. 8. Cross correlation of the input variables.

Table 2
Points of min and max cross correlation between the lagged features and the target (FP).

Feature	$Lag_M Corr$	$MaxCorrelation$	$Lag_m Corr$	$MinCorrelation$
ET_o	8	0.492	21	−0.527
Hour_sin	1	0.554	13	−0.553
IR	8	0.147	18	0.006
K_c	24	0.204	0	0.187
P	17	0.032	6	−0.021
RH	0	0.494	11	−0.364
Rs	8	0.506	20	−0.509
SWC	0	0.555	16	0.380
T	11	0.348	0	−0.567
U	11	0.336	23	−0.456
VPD	10	0.351	0	−0.550

Table 3
The final selected hyperparameters for the optimal models without using previous TWP lags.

Algorithm	Parameter	Value
RF	n_estimators	300
	max_depth	15
KNN	n_neighbors	7
	weights	Distance
	algorithm	Auto
SVR	C	10
	epsilon	0.1
	kernel	Poly
LSTM	Embedding dimension	12
	LSTM units (1st layer)	128
	LSTM units (2nd layer)	64
	Learning rate	0.00147

Table 4
Model evaluation results of the ML and DL models in predicting TWP values for the next hour.

Algorithm	Tree	R2	MAE (MPa)	RMSE (MPa)	CVRMSE (%)
RF	T1.1.	0.645	0.200	0.237	21.152
	T1.2.	0.579	0.186	0.232	17.248
	T2.1.	0.496	0.281	0.356	23.521
	T2.2.	0.556	0.171	0.201	16.006
	T3.1.	0.292	0.198	0.240	21.634
	T4.1.	0.715	0.313	0.374	33.544
	T4.2.	0.695	0.186	0.231	21.579
	Average	0.568	0.219	0.267	22.098
KNN	T1.1.	0.584	0.177	0.219	19.493
	T1.2.	0.622	0.208	0.256	19.047
	T2.1.	0.553	0.255	0.319	21.078
	T2.2.	0.567	0.173	0.211	16.775
	T3.1.	0.525	0.187	0.233	20.983
	T4.1.	0.630	0.324	0.384	34.453
	T4.2.	0.710	0.150	0.181	16.933
	Average	0.599	0.211	0.258	21.251
SVR	T1.1.	0.397	0.182	0.234	20.829
	T1.2.	0.424	0.230	0.290	21.551
	T2.1.	0.433	0.267	0.362	23.957
	T2.2.	0.514	0.189	0.243	19.308
	T3.1.	0.429	0.195	0.243	21.891
	T4.1.	0.532	0.323	0.385	34.514
	T4.2.	0.617	0.155	0.197	18.427
	Average	0.478	0.220	0.279	22.925
LSTM	T1.1.	0.612	0.211	0.260	23.175
	T1.2.	0.713	0.158	0.204	15.170
	T2.1.	0.748	0.193	0.237	15.673
	T2.2.	0.768	0.203	0.235	18.660
	T3.1.	0.775	0.119	0.148	13.314
	T4.1.	0.805	0.297	0.353	31.678
	T4.2.	0.861	0.155	0.180	16.883
	Average	**0.754**	**0.191**	**0.231**	**19.222**

4.2. Models with TWP lags

To generate results that incorporate TWP lags, we structured the analysis based on the assumption that 12 previous lags of TWP measurements are necessary. This decision is supported by the approximately 24-hour physiological cycles observed in the TWP data. In addition, we established 1-hour, 6-hour, 12-hour, and 24-hour prediction horizons for the evaluation. The general structure of the data and the target prediction setup are illustrated in Fig. 9.

The reason for selecting these specific horizons is twofold. First, longer prediction horizons do not provide meaningful information, as irrigation strategies typically take effect within 6-8 h. To avoid unnecessary stress, a horizon longer than 6 h should be sufficient to adjust irrigation strategies. Second, as the prediction horizon increases, the associated error tends to grow, so shorter horizons are more reliable and preferable.

To balance predictive ability and practical utility, we chose a set of prediction horizons of [1 h, 6 h, 12 h, 24 h]. In addition, traditional ML models were discarded in this analysis, since adding more variables increases noise, and these models are very susceptible to such perturbations. Instead, LSTM demonstrated a strong ability to capture complex relationships within the data, making it a more suitable approach for this type of prediction. Also, for multi-horizon predictions, the models use the same set of input features, including observed lagged TWP values up to the maximum lag defined. Forecasts for each horizon are generated independently (direct forecasting), and model predictions are not recursively used as inputs for subsequent predictions.

The final values of the hyperparameters for each LSTM model are listed in Table 5. Fig. 11 shows the four model evaluation results over different time horizons. Comparing the models, it is clear that for the same steps, except for 4, 5 and 6 with the 6H model, a shorter prediction horizon always gave better results than those with longer horizons. Specifically for the first step, the 1H model gave the best performance in all metrics, with R^2 = 0.983, MAE = 0.036 MPa, RMSE = 0.049 MPa and CVRMSE = 3.997%. A similar trend can be seen for all metrics. For the first step, a large decrease can be observed from

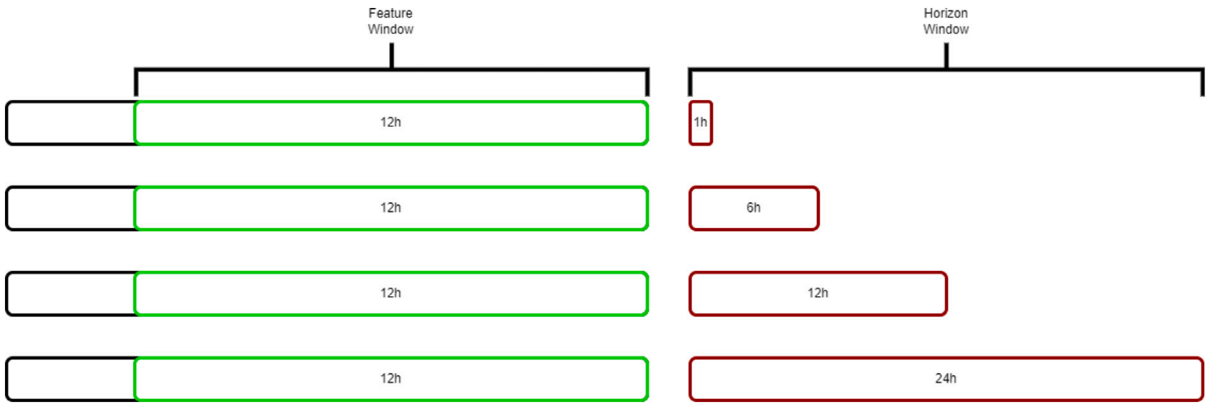

Fig. 9. Windows size and horizon size.

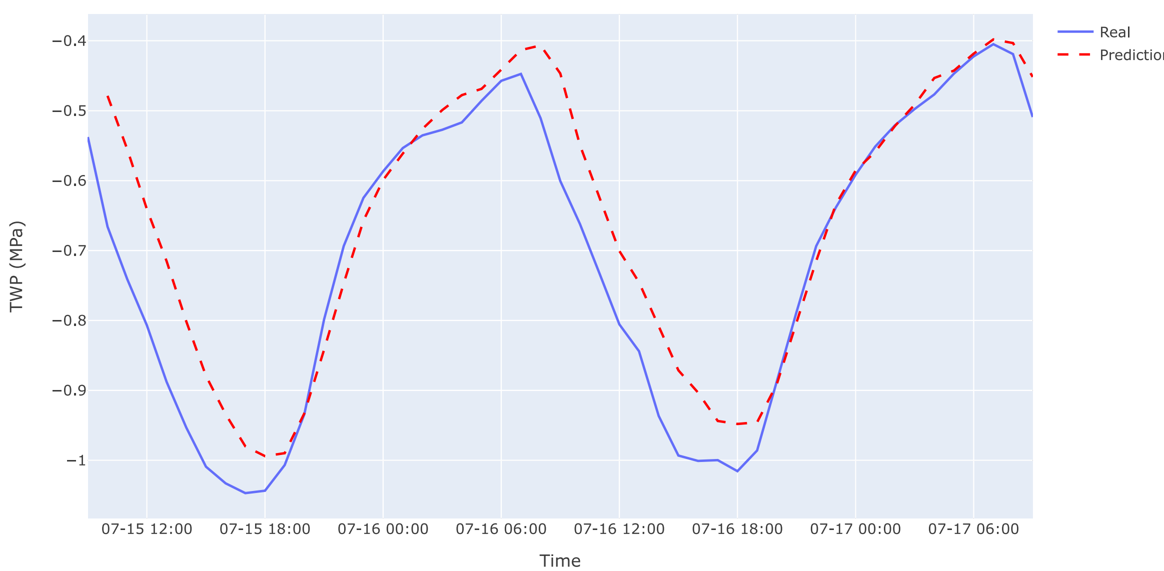

Fig. 10. Comparison between observed and predicted TWP for the 24-hour forecasting model over a 48-hour period, starting at 2023-07-15 09:00:00 for the tree T3.1.

Table 5
The final selected hyperparameters for the optimal LSTM models using previous TWP lags at different horizons.

Horizon	Parameter	Value
1H	Embedding dimension	4
	LSTM units (1st layer)	96
	LSTM units (2nd layer)	24
	Learning rate	0.00119
6H	Embedding dimension	4
	LSTM units (1st layer)	96
	LSTM units (2nd layer)	52
	Learning rate	0.00292
12H	Embedding dimension	12
	LSTM units (1st layer)	72
	LSTM units (2nd layer)	60
	Learning rate	0.00412
24H	Embedding dimension	8
	LSTM units (1st layer)	128
	LSTM units (2nd layer)	64
	Learning rate	0.00275

the 1H model to the remaining models. The main reason is that the 1H model only focuses on learning the prediction for the next step, and the other models have to learn to predict multiple steps at the same time, and therefore the performance variation of multi-step models is very small and gradual as the horizon increases. Remarkably, the 24H model showed a contradiction where steps 17 to 23 had better performance than step 16. We interpret this is because when the prediction of the 24H horizon includes both day and night values, where normally the values of TWP are more stable at night and it helps the model to predict more accurate values.

To better illustrate the behavior of the 24H forecasting model, Fig. 10 presents an example comparison between observed and predicted TWP values over a 48-hour period. Since the model generates a new 24-hour forecast at each time step, the prediction windows overlap. This makes it difficult to represent long, continuous forecast trajectories without ambiguity. For visualization purposes, the 24-hour forecast trajectories generated for two consecutive days were concatenated, resulting in a 48-hour comparison window.

The example shown (starting at 2023-07-15 09:00:00 for the tree T3.1.) illustrates the behavior discussed above: the model tends to produce more accurate predictions during nighttime periods, when TWP values remain relatively stable, while larger deviations may occur during daytime periods characterized by stronger atmospheric forcing. Similar patterns were observed for several other days/trees, although this behavior is not systematic.

On the other hand, Table 6 presents the average results of the four metrics. At 1H, the model had the best performance, as shown before. As the horizon increases, all the error metrics (MAE, RMSE, and CVRMSE) increase, while R^2 decreases, indicating a drop in the model's ability to explain the variance in the data. At 6H, 12H, and

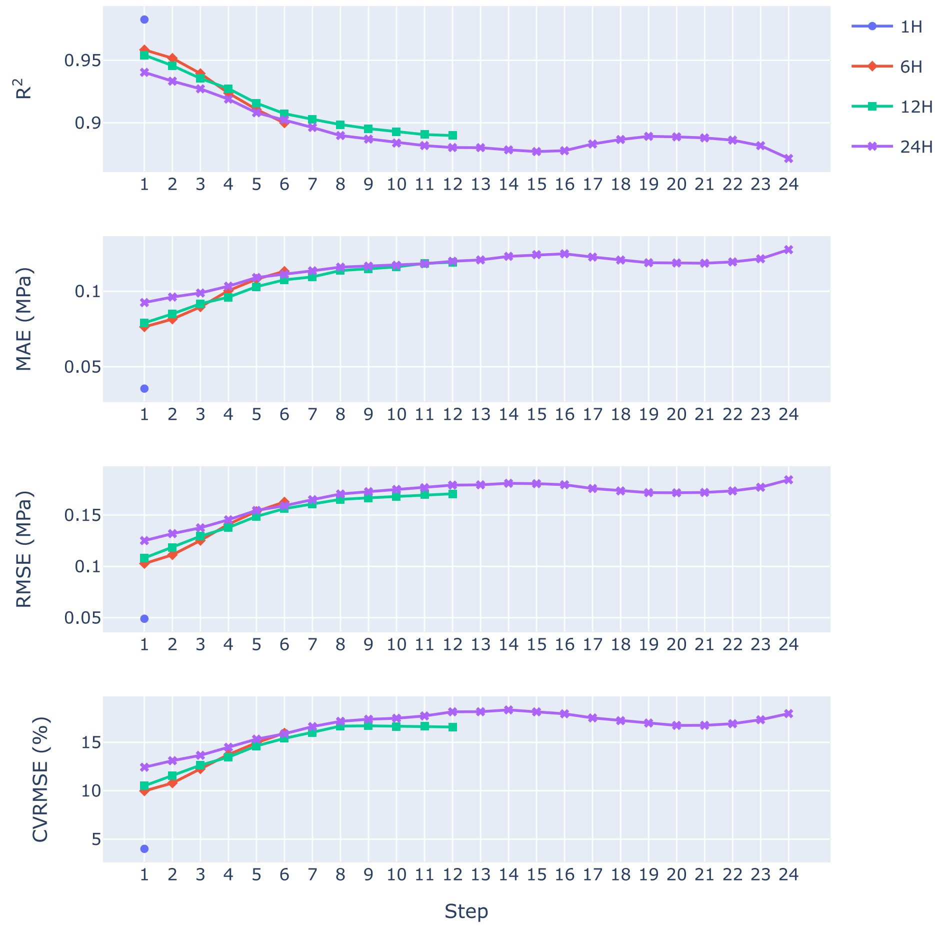

Fig. 11. Four performance metrics of prediction from 1 to 24 h horizon by LSTM model.

Table 6
Model evaluation results of the LSTM models in predicting TWP values from 1 to 24 h ahead. Each metric is calculated as the average of all trees and all steps.

Horizon	R2	MAE (MPa)	RMSE (MPa)	CVRMSE (%)
1H	0.983	0.036	0.049	3.997
6H	0.931	0.095	0.133	12.948
12H	0.913	0.105	0.150	14.790
24H	0.893	0.116	0.167	16.647

24H, the R^2 of the model progressively decreases (from 0.983 to 0.893) and the errors increase, meaning that both the prediction error (MAE from 0.036 MPa to 0.0116 MPa and RMSE from 0.049 to 0.167 MPa) and the relative error (CVRMSE from 3.997% to 16.647%) increase significantly for longer-term predictions. Overall, the LSTM model performs very well for short-term predictions, but its accuracy degrades as the prediction horizon lengthens. This is to be expected for time series predictions as uncertainty increases with time.

5. Discussion

5.1. Improvements over the previous study

Compared to the previous study, the earlier approach of integrating TWP sensors with traditional ML had several key limitations. First, some of the data comparison relied heavily on Mean Absolute Percentage Error (MAPE) as the primary evaluation metric. However, MAPE is known to be unsuitable for data sets containing negative values, as is the case for TWP measurements, leading to misleading performance evaluations. Second, the previous methodology was only tested on a limited number of trees, which restricted its generalizability and robustness under different tree conditions. Finally, the significance of the variables was mainly attributed to the lagged TWP values, without taking into account the contribution of climatic and irrigation characteristics.

Given these limitations, the new methodology implements several significant improvements to increase the robustness, interpretability and practical application of the model:

1. **Expanded Dataset Scope and one model for all trees**: Unlike the previous method, which focused on a small number of trees, the updated approach evaluates all available trees to test the robustness of the model. In addition, a single model is trained using all available trees and is capable of predicting any of them, whereas in the previous study a unique tree was used to train a single model and validate it on other trees. This broader validation ensures that models generalize well under different conditions, making them more reliable for real-world applications.
2. **Comprehensive data and model analysis**: To address the previous over-reliance on lagged TWP values, the new methodology follows a two modeling approach:
   (a) Excludes lagged TWP variables to allow climatic and irrigation-related characteristics to play a more significant role. This configuration ensures that future irrigation optimization strategies can be developed independently of TWP readings, making the system more versatile.

Table 7
Performance metrics of old models for different trees.

Model	T1.1			T2.1			T4.2		
	R^2	MAE (bar)	MAPE (%)	R^2	MAE (bar)	MAPE (%)	R^2	MAE (bar)	MAPE (%)
SVR	0.751	1.813	17.762	0.804	2.340	19.053	0.749	1.890	41.63
RF	**0.899**	**1.170**	**12.628**	**0.966**	**1.158**	**8.793**	**0.944**	**1.019**	**29.620**
KNN	0.769	1.784	18.532	0.907	1.781	15.096	0.753	1.906	48.14

(b) Incorporates lagged TWP values but applies models capable of handling the complex interactions within the data. In this regard, LSTM was selected as the preferred model due to its superior ability to capture intricate temporal dependencies.

Comparing both results, it can be concluded that the inclusion of lagged values certainly improves the model performance (R^2 increased from 0.754 to 0.983 and CVRMSE decreased from 19.222% to 3.997%). The main disadvantage of using lagged values is that previous TWP values must be available as input and they will always be the most important variable to make the prediction.

3. **Extended Prediction Horizons**: The new framework extends the prediction horizon from one hour to 24 h. This improvement allows for more practical irrigation scheduling as irrigation strategies typically take effect within 6-8 h.

Together, these improvements result in a more adaptable and informative system for precision irrigation. Expanding the data set, refining modeling strategies, and increasing prediction horizons ensure that the new approach is more reliable and applicable to a variety of agricultural settings.

Regarding the comparison of the metrics of the old study with those of the new study, it is important to note that it is not possible to make a direct comparison with the models without time lag, as the models of the old version only worked with time lag. Furthermore, it is important to note that the climate and irrigation variables were not lagged over a 12-hour period. Therefore, it is recommended to make the comparison with the LSTM model and, in addition, to examine that, by lagging the variables, it is possible to obtain other equally efficient models, although the use of the LSTM models is advised due to their optimal performance under similar conditions.

The comparison between Tables 7 and 4 tables highlights the key improvements achieved with the new methodology. In particular, better results have been obtained even without using lagged variables, especially with the LSTM model, demonstrating its ability to effectively capture temporal dependencies.

In addition, the elimination of lagged variables has increased the relative importance of other factors, as seen in the improved performance of the RF model. This improvement allows for a more detailed future study on how irrigation strategies and climatic conditions affect plant stress, which will ultimately lead to more efficient irrigation and cultivation techniques. It can also be observed that the incorporation of lagged variables in the short-term predictions (1 h) with LSTM (Table 6) further improves the results, not only for specific trees but in all cases.

5.2. Comparison with other studies

In the field of TWP/SWP prediction, ML techniques are still not widely explored. In particular, the first FloraPulse MT system was sold in 2018. Therefore, as novel methods, similar studies are limited. In the study of Savchik et al. [51], SWP maps in a almond orchard were predicted based on canopy spectral reflectance, soil moisture, and daily ET_o. With ANN and RF models, they achieved in an average coefficient of correlation of $R^2 = 0.73$ and an average RMSE of 2.5 bars. Mortazavi et al. [34] used weather, thermal and multispectral data as inputs to estimate SWP. Six ML models were implemented as classifiers to determine the water status and RF was used to predict exact values of SWP. With all available data, the RF model achieved 0.70 in R^2, 1.13 bar in RMSE and 0.84 bar in MAE. Compared to our results, our models perform less effectively when using only weather data. However, when previous TWP values are included, our LSTM models outperform the corresponding RF in all metrics ($R^2 = 0.983$, RMSE = 0.49 bar and MAE = 0.36 bar). It should be noted that the mentioned studies estimate the TWP, whereas our methodology forecasts the future TWP values.

Some of the studies addressed the problem as a classification problem [18,34,35]. Classifiers prioritize grouping data into categories (severe, mild and no water stress or irrigate/not to irrigate) instead of predicting precise values, leading to higher accuracy and increased robustness to noise. However, by capturing continuous variation and the exact output values, regression models can improve the accuracy of irrigation decisions and enable a more precise and scalable solution for sustainable orchard water management.

It is also important to note that, beyond predictive performance, the evaluated models present different trade-offs that are relevant for practical deployment. Simpler approaches, such as KNN and SVR, offer lower computational costs and easier implementation. This makes them suitable for real-time or resource-constrained environments. In contrast, more complex models, such as LSTMs, are better suited to capturing temporal dependencies and nonlinear dynamics, despite higher computational requirements and reduced interpretability. Ensemble methods, such as RF, provide a balance between accuracy and robustness, offering stable performance across different conditions.

From a practical perspective, the choice of model should consider factors such as computational efficiency, scalability, and ease of integration into decision-support systems, in addition to prediction accuracy.

5.3. Limitations and applicability of the proposed approach

The dataset used in this study covers the 2023 season, during which the plot treatments were maintained with full irrigation (100% ETc). Consequently, the model learned to map climate, soil moisture, irrigation, and previous TWP observations to future TWP within the domain of well-watered conditions. The model largely reflects the baseline diurnal and seasonal dynamics present during that campaign.

However, it is important to note that the model has not been exposed to the physiological responses trees exhibit under water stress (e.g., larger negative TWP excursions, altered hysteresis between environmental drivers and TWP, and non-linear responses across phenological stages) because the training data do not include controlled or natural water deficit scenarios. Consequently, while the model may perform well when interpolating within the range of observed (well-watered) TWP values, it could systematically under- or overestimate TWP under deficit irrigation or fail to capture stress-specific dynamics.

To address the limitations associated with the absence of drought-stressed observations, ongoing work is focused on expanding the dataset to include a wider range of plant water status conditions. In particular, the experimental campaign conducted during the 2024 and 2025 growing seasons incorporated different irrigation strategies, including deficit irrigation treatments, with the objective of inducing controlled variations in tree water status. These experiments were designed specifically to capture TWP dynamics under both well-watered and water-limited conditions, thereby extending the range of physiological responses represented in the dataset. The data collected during this campaign are currently being organized and processed, and will provide valuable information to retrain and validate the predictive models under a broader spectrum of irrigation scenarios. Incorporating these data will allow the models to learn not only the baseline climate-driven diurnal patterns observed under optimal irrigation, but also the non-linear physiological responses associated with water deficit. Consequently, future model versions will be able to better capture stress-related dynamics and more reliably support irrigation management decisions.

Finally, this study focuses on peach trees due to the availability of a well-instrumented experimental orchard. Nevertheless, the proposed machine learning framework is not inherently crop-specific. The methodology aims to identify relationships among environmental conditions, irrigation inputs, soil variables, and plant water status. Therefore, it could be applied to other crops, provided suitable physiological measurements are available.

However, the FloraPulse microtensiometers used in this study require installation inside the trunk, which may not be feasible or desirable for all tree species or agricultural contexts. As mentioned in the experimental setup, proper sensor installation is also critical for accurate measurements. Consequently, future work could explore integrating alternative plants into the same modeling framework. This would allow the proposed approach to be applied to a wider range of crops and agricultural systems.

6. Conclusion

In this study, significant progress has been made in the development of tools for irrigation management in peach crops by estimating TWP using sensor data; FloraPulse MT, climatic variables, SWC and indices such as K_c. In this second phase of the project, the extension of the DL model's predictive horizon to 24 h provides an improved ability to anticipate water stress and adjust irrigation strategies based on future conditions, maximizing water use efficiency. The first comparison between the standard ML (RF, KNN, and SVR) and DL (LSTM) models, without using previous TWP values, showed that LSTM outperformed the other models with less than 20% of CVRMSE. At broader horizons (from 1 to 24 h) and using TWP lags, the LSTM model demonstrated excellent performance with a gradual increase in errors (from 4% to 17% of CVRMSE).

It should be noted that the implemented models used data from the 2023 season, during which all trees were irrigated at 100% of ET_c to ensure optimal and homogeneous conditions in the initial evaluation. In order to further validate the generalizability of the developed model, data from the 2024 campaign will be used, where different irrigation strategies will be applied.

In addition, the predictive models developed in this study are relevant and will be integrated into a broader digital platform currently under development. The goal of this platform is to evolve into an Marine-Agricultural Digital Twin framework that can combine predictive models, real-time sensor data, and environmental information to simulate crop water dynamics and evaluate irrigation management scenarios. In this context, the models presented here can support *what-if* analyses related to irrigation strategies and water use, especially in regions with limited water resources, such as the Murcia Region in southeastern Spain.

6.1. Future perspectives

Considering that the real-time TWP data and the mathematical model obtained allow for better irrigation management, further research is essential to:

- Define accurate TWP threshold values that serve as a reference for an efficient decision support system.
- Evaluate the long-term stability and performance of FloraPulse MTs, ensuring consistency of measurements under varying conditions.
- Incorporate additional variables, including metrics related to the quantity and quality of the harvest, to further improve irrigation decisions.
- Apply Transfer Learning (TL) techniques to improve the generalizability of the models in diverse agricultural environments [52].
- Incorporate explainable AI techniques to improve model interpretability.

Furthermore, the integration of ML models allows accurate prediction of future FloraPulse values. The next step is to apply optimization algorithms to determine the minimum amount of water required at each irrigation event, ensuring that the predicted FloraPulse values remain within a set range. This will achieve the ultimate goal of determining precisely when and how much to irrigate, optimizing water use and improving the sustainability of agricultural production.

CRediT authorship contribution statement

Yu Ye: Writing – review & editing, Writing – original draft, Software, Investigation, Conceptualization. **María Fernanda García Cruz:** Writing – review & editing, Writing – original draft, Validation, Investigation, Conceptualization. **Ricardo Javier Sendra Lázaro:** Writing – review & editing, Writing – original draft, Software, Data curation. **Miguel A. Zamora-Izquierdo:** Writing – review & editing, Methodology, Conceptualization. **Aurora González-Vidal:** Writing – review & editing, Validation, Methodology. **Pedro Nortes Tortosa:** Writing – review & editing, Resources, Methodology. **José Salvador Rubio-Asensio:** Writing – review & editing, Resources, Methodology. **María Fernanda Ortuño Gallud:** Writing – review & editing, Resources, Methodology. **Antonio F. Skarmeta:** Writing – review & editing, Resources, Project administration, Funding acquisition.

Declaration of competing interest

The authors declare that they have no known competing financial interests or personal relationships that could have appeared to influence the work reported in this paper.

Acknowledgments

This study was supported by grant RYC2023-043553-I, funded by MICIU/AEI/10.13039/501100011033 and ESF+ as well as the HORIZON-MSCA-2021-SE-01-01 project Cloudstars (g.a. 101086248) and FEDER/EU. It was also supported by the projects of the Innovation Spanish Agency: EDEN (CPP2021-009146) as well as by projects GEMINI (TED2021-129767B-I00), OSIRIS (TSI-100921-2023-1 Cátedras ENIA), NEMESIS (the Horizon Europe project, Grant Agreement No. 101219087), and financed by DEMETER 5.0 (PLEC2022-009289).

References

[1] FAO, El estado mundial de la agricultura y la alimentación 2020. Superar los desafíos relacionados con el agua en la agricultura, 2020, URL: https://doi.org/10.4060/cb1447es.

[2] E. Fereres, M.A. Soriano, Deficit irrigation for reducing agricultural water use, J. Exp. Bot. 58 (2) (2007) 147–159.

[3] I. Fernández García, S. Lecina, M.C. Ruiz-Sánchez, J. Vera, W. Conejero, M.R. Conesa, A. Domínguez, J.J. Pardo, B.C. Léllis, P. Montesinos, Trends and challenges in irrigation scheduling in the semi-arid area of Spain, Water 12 (3) (2020) 785.

[4] C. Varela-Ortega, I. Blanco-Gutiérrez, P. Esteve, S. Bharwani, S. Fronzek, T.E. Downing, How can irrigated agriculture adapt to climate change? Insights from the Guadiana Basin in Spain, Reg. Environ. Chang. 16 (2016) 59–70.

[5] N. Katerji, M. Mastrorilli, G. Rana, Water use efficiency of crops cultivated in the Mediterranean region: Review and analysis, Eur. J. Agron. 28 (4) (2008) 493–507.

[6] P.y.A. Ministerio de agricultura, Anuario de estadística 2023, 2023, URL: https://www.mapa.gob.es/.
[7] A. Carella, P.T. Bulacio Fischer, R. Massenti, R. Lo Bianco, Continuous plant-based and remote sensing for determination of fruit tree water status, Horticulturae 10 (5) (2024) 516.
[8] A. Fernandes-Silva, M. Oliveira, T.A. Paço, I. Ferreira, Deficit Irrigation in Mediterranean Fruit Trees and Grapevines: Water Stress Indicators and Crop Responses, vol. 24, IntechOpen London, UK, 2018.
[9] J.E. Fernández, Plant-based methods for irrigation scheduling of woody crops, Horticulturae 3 (2) (2017) 35.
[10] H. Jones, Irrigation scheduling–comparison of soil, plant and atmosphere monitoring approaches, in: V International Symposium on Irrigation of Horticultural Crops 792, 2006, pp. 391–403.
[11] G. Noun, M. Lo Cascio, D. Spano, S. Marras, C. Sirca, Plant-based methodologies and approaches for estimating plant water status of Mediterranean tree species: a semi-systematic review, Agronomy 12 (9) (2022) 2127.
[12] P.F. Scholander, E.D. Bradstreet, E. Hemmingsen, H. Hammel, Sap pressure in vascular plants: Negative hydrostatic pressure can be measured in plants, Science 148 (3668) (1965) 339–346.
[13] K. Steppe, D.J. De Pauw, R. Lemeur, A step towards new irrigation scheduling strategies using plant-based measurements and mathematical modelling, Irrig. Sci. 26 (2008) 505–517.
[14] A.N. Lakso, M. Santiago, A.D. Stroock, Monitoring stem water potential with an embedded microtensiometer to inform irrigation scheduling in fruit crops, Horticulturae 8 (12) (2022) 1207.
[15] M. Javaid, A. Haleem, I.H. Khan, R. Suman, Understanding the potential applications of artificial intelligence in agriculture sector, Adv. Agrochem 2 (1) (2023) 15–30.
[16] M.F.G. Cruz, Y. Ye, M.F.O. Gallud, R.J.S. Lázaro, M.A.Z. Izquierdo, P.N. Tortosa, A.S. Gómez, Creation of a digital twin based on microtensiometer indices (Florapulse), climatic variables and crop data for sustainable production in stone fruit crops, in: 2024 4th International Conference on Embedded & Distributed Systems, EDiS, IEEE, 2024, pp. 243–248.
[17] Y. Ye, A. González-Vidal, A. Cisterna-García, A. Pérez-Ruzafa, M.A.Z. Izquierdo, A.F. Skarmeta, Advancing towards a marine digital twin platform: Modeling the Mar Menor coastal lagoon ecosystem in the south western Mediterranean, Future Gener. Comput. Syst. (2025) 108265.
[18] J.A. Barriga, F. Blanco-Cipollone, E. Trigo-Córdoba, I. García-Tejero, P.J. Clemente, Crop-water assessment in citrus (Citrus sinensis L.) based on continuous measurements of leaf-turgor pressure using machine learning and IoT, Expert Syst. Appl. 209 (2022) 118255.
[19] V. Blanco, L. Kalcsits, Microtensiometers accurately measure stem water potential in woody perennials, Plants 10 (12) (2021) 2780.
[20] V. Blanco, L. Kalcsits, Long-term validation of continuous measurements of trunk water potential and trunk diameter indicate different diurnal patterns for pear under water limitations, Agricult. Water. Manag. 281 (2023) 108257.
[21] M.R. Conesa, W. Conejero, J. Vera, M.C. Ruiz-Sánchez, Assessment of trunk microtensiometer as a novel biosensor to continuously monitor plant water status in nectarine trees, Front. Plant Sci. 14 (2023) 1123045.
[22] H. McCutchan, K. Shackel, Stem-water potential as a sensitive indicator of water stress in prune trees (prunus domestica l. cv. French), 1992.
[23] A. Naor, Midday stem water potential as a plant water stress indicator for irrigation scheduling in fruit trees, in: III International Symposium on Irrigation of Horticultural Crops 537, 1999, pp. 447–454.
[24] B. Suter, R. Triolo, D. Pernet, Z. Dai, C. Van Leeuwen, Modeling stem water potential by separating the effects of soil water availability and climatic conditions on water status in grapevine (Vitis vinifera L.), Front. Plant Sci. 10 (2019) 1485.
[25] J. Bellvert, P.J. Zarco-Tejada, J. Marsal, J. Girona, V. González-Dugo, E. Fereres, Vineyard irrigation scheduling based on airborne thermal imagery and water potential thresholds, Aust. J. Grape Wine Res. 22 (2) (2016) 307–315.
[26] A. Boini, L. Manfrini, G. Bortolotti, L. Corelli-Grappadelli, B. Morandi, Monitoring fruit daily growth indicates the onset of mild drought stress in apple, Sci. Hort. 256 (2019) 108520.
[27] M.R. Conesa, W. Conejero, J. Vera, J.M. Ramírez-Cuesta, M.C. Ruiz-Sánchez, Terrestrial and remote indexes to assess moderate deficit irrigation in early-maturing nectarine trees, Agronomy 9 (10) (2019) 630.
[28] V. Pagay, Evaluating a novel microtensiometer for continuous trunk water potential measurements in field-grown irrigated grapevines, Irrig. Sci. 40 (1) (2022) 45–54.
[29] V. Pagay, M. Santiago, D.A. Sessoms, E.J. Huber, O. Vincent, A. Pharkya, T.N. Corso, A.N. Lakso, A.D. Stroock, A microtensiometer capable of measuring water potentials below- 10 MPa, Lab A Chip 14 (15) (2014) 2806–2817.
[30] L. González, A. Huber, R. Gao, L. Cheng, A. Stroock, A. Lakso, T. Robinson, Using micro-tensiometers to manage water stress to maximize fruit size of apple orchards, in: XXXI International Horticultural Congress (IHC2022): International Symposium on Water: A Worldwide Challenge for Horticulture! 1373, 2022, pp. 113–120.
[31] I. Kisekka, S.R. Peddinti, P. Savchik, L. Yang, M. Culumber, K. Bali, L. Milliron, E. Edwards, M. Nocco, C.A. Reyes, et al., Multisite evaluation of microtensiometer and osmotic cell stem water potential sensors in almond orchards, Comput. Electron. Agric. 227 (2024) 109547.
[32] C. Hernandez-Hidalgo, A. González-Vidal, A.F. Skarmeta, Enhancing precision irrigation with TinyML: Advanced NDVI anomaly detection and model optimization, Internet Things (2025) 101839.
[33] S. Violino, S. Figorilli, M. Ferrigno, V. Manganiello, F. Pallottino, C. Costa, P. Menesatti, A data-driven bibliometric review on precision irrigation, Smart Agric. Technol. 5 (2023) 100320.
[34] M. Mortazavi, S. Carpin, A. Toudeshki, R. Ehsani, A practical data-driven approach for precise stem water potential monitoring in pistachio and almond orchards using supervised machine learning algorithms, Comput. Electron. Agric. 231 (2025) 110004.
[35] F. Salek, S.A. Mireei, A. Hemmat, M. Jafari, M.R. Sabzalian, M. Nazeri, W. Saeys, Early monitoring of drought stress in safflower (Carthamus tinctorius L.) using hyperspectral imaging: A comparison of machine learning tools and feature selection approaches, Plant Stress. 14 (2024) 100653.
[36] R.G. Allen, L.S. Pereira, D. Raes, M. Smith, et al., Crop evapotranspiration-guidelines for computing crop water requirements-FAO irrigation and drainage paper 56, Fao, Rome 300 (9) (1998) D05109.
[37] J. Girona, M. Gelly, M. Mata, A. Arbones, J. Rufat, J. Marsal, Peach tree response to single and combined deficit irrigation regimes in deep soils, Agricult. Water. Manag. 72 (2) (2005) 97–108.
[38] W.L. Black, M. Santiago, S. Zhu, A.D. Stroock, Ex situ and in situ measurement of water activity with a MEMS tensiometer, Anal. Chem. 92 (1) (2019) 716–723.
[39] A. Lakso, S. Zhu, M. Santiago, K. Shackel, V. Volkov, A. Stroock, A microtensiometer sensor to continuously monitor stem water potentials in woody plants design and field testing, in: IX International Symposium on Irrigation of Horticultural Crops 1335, 2019, pp. 317–324.
[40] L.F.R. Sánchez, La práctica de la fertirrigación en el cultivo del melocotonero, Vida Rural. (307) (2010) 68–72.
[41] M. Rahimzad, A. Moghaddam Nia, H. Zolfonoon, J. Soltani, A. Danandeh Mehr, H.-H. Kwon, Performance comparison of an LSTM-based deep learning model versus conventional machine learning algorithms for streamflow forecasting, Water Resour. Manag. 35 (12) (2021) 4167–4187.
[42] S. Bouktif, A. Fiaz, A. Ouni, M.A. Serhani, Optimal deep learning lstm model for electric load forecasting using feature selection and genetic algorithm: Comparison with machine learning approaches, Energies 11 (7) (2018) 1636.
[43] F. Chollet, et al., Keras, 2015, https://github.com/fchollet/keras. Accedido: 2024-02-24.
[44] F. Pedregosa, G. Varoquaux, A. Gramfort, V. Michel, B. Thirion, O. Grisel, M. Blondel, P. Prettenhofer, R. Weiss, V. Dubourg, J. Vanderplas, A. Passos, D. Cournapeau, M. Brucher, M. Perrot, E. Duchesnay, Scikit-learn: Machine learning in python, J. Mach. Learn. Res. 12 (2011) 2825–2830.
[45] L. Breiman, Random forests, Mach. Learn. 45 (2001) 5–32.
[46] C. Cortes, V. Vapnik, Support-vector networks, Mach. Learn. 20 (1995) 273–297.
[47] J.A. Bellido-Jiménez, J. Estévez, A.P. García-Marín, New machine learning approaches to improve reference evapotranspiration estimates using intra-daily temperature-based variables in a semi-arid region of Spain, Agricult. Water. Manag. 245 (2021) 106558.
[48] T. Cover, P. Hart, Nearest neighbor pattern classification, IEEE Trans. Inform. Theory 13 (1) (1967) 21–27.
[49] J. Schmidhuber, S. Hochreiter, et al., Long short-term memory, Neural Comput. 9 (8) (1997) 1735–1780.
[50] C. Brouwer, K. Prins, M. Kay, M. Heibloem, Irrigation water management: irrigation methods, Train. Man. 9 (5) (1988) 5–7.
[51] P. Savchik, M. Nocco, I. Kisekka, Mapping almond stem water potential using machine learning and multispectral imagery, Irrig. Sci. 43 (1) (2025) 105–120.
[52] Y. Ye, A. González-Vidal, M.A. Zamora-Izquierdo, A.F. Skarmeta, Transfer and deep learning models for daily reference evapotranspiration estimation and forecasting in Spain from local to national scale, Smart Agric. Technol. (2025) 100886.